INTERNATIONAL JOURNAL OF CLIMATOLOGY
Int. J. Climatol. (2011)
Published online in Wiley Online Library
(wileyonlinelibrary.com) DOI: 10.1002/joc.2390

RMetS
Royal Meteorological Society

High-resolution (space, time) anthropogenic heat emissions: London 1970–2025

Mario Iamarino,[a]* Sean Beevers[b] and C. S. B. Grimmond[c]

[a] *Dipartimento di Ingegneria e Fisica dell'Ambiente, Università degli Studi della Basilicata, via dell'Ateneo Lucano 10, 85100 Potenza, Italy*
[b] *Environmental Research Group, King's College London, Franklin-Wilkins Building, 150 Stamford Street, London SE1 9NH, UK*
[c] *Environmental Monitoring and Modelling Group, Department of Geography, King's College London, The Strand, London WC2R 2LS, UK*

ABSTRACT: The anthropogenic heat emissions generated by human activities in London are analysed in detail for 2005–2008 and considered in context of long-term past and future trends (1970–2025). Emissions from buildings, road traffic and human metabolism are finely resolved in space (30 min) and time (200×200 m^2). Software to compute and visualize the results is provided. The annual mean anthropogenic heat flux for Greater London is 10.9 W m^{-2} for 2005–2008, with the highest peaks in the central activities zone (CAZ) associated with extensive service industry activities. Towards the outskirts of the city, emissions from the domestic sector and road traffic dominate. Anthropogenic heat is mostly emitted as sensible heat, with a latent heat fraction of 7.3% and a heat-to-wastewater fraction of 12%; the implications related to the use of evaporative cooling towers are briefly addressed. Projections indicate a further increase of heat emissions within the CAZ in the next two decades related to further intensification of activities within this area. Copyright © 2011 Royal Meteorological Society

KEY WORDS anthropogenic heat; London; heat emissions; sensible heat; latent heat; energy consumption

Received 11 February 2011; Revised 20 May 2011; Accepted 3 June 2011

1. Introduction

Thermal pollution is the emission to the environment of large amounts of waste heat associated with human activities. It is recognized as a contributor to the urban heat island (UHI) effect, where cities experience higher air temperatures relative to contiguous rural areas. Elevated urban temperatures result in increased summertime mortality rates under heat wave conditions, higher summer energy consumption for cooling, which may increase further the UHI intensity, and changes in atmospheric chemistry and phenology (Zhang *et al*., 2004). Quantitative and qualitative characterization of urban anthropogenic heat emissions have been recently reviewed by Sailor (2011) and treated in numerical models in a wide range of ways (Grimmond *et al*., 2010).

The anthropogenic heat flux Q_F (W m^{-2}) is the rate at which waste energy is discharged by human activities to the surroundings. The three main contributions to total Q_F are: the heat flux deriving from energy consumption in buildings ($Q_{F,B}$), from the transportation sector ($Q_{F,T}$) and from human metabolism ($Q_{F,M}$) (Grimmond, 1992)

$$Q_F = Q_{F,B} + Q_{F,T} + Q_{F,M} \quad (1)$$

Three general approaches have been recognized to estimate these terms (Sailor, 2011): the use of statistics on energy consumption (Hamilton *et al*., 2009), the closure of the energy budget (Offerle *et al*., 2005) and, for the building sector, the building energy modelling approach (Kikegawa *et al*., 2003). Another distinction can be made based on the fluxes determined: total (aggregated sensible plus latent), only sensible or sensible and latent separately. The latent heat flux accounts in summer for about 25% of total Q_F in central Tokyo (Moriwaki *et al*., 2008), and similar results are found in Houston, TX, USA (Sailor *et al*., 2007). For the Osaka Prefecture, Narumi *et al*. (2009) found the sensible heat, latent heat and heat-to-wastewater to be 61, 23 and 16% of total Q_F, respectively. In these cases, the main contributors to latent heat emissions are evaporative towers used in large cooling systems.

A further classification relates to how energy discharge is treated. As shown in Figure 1, discharge from transportation is directly into the atmosphere and without significant time lag. As a consequence, profiles of energy generation from road fuels and atmospheric heat emissions are coincident in practice, and the same applies to metabolic emissions from people outdoors. This is not true for the energy consumed in buildings and the metabolic emissions from people within because of the heat transfer resistance (R_1) between buildings and atmosphere and the thermal inertia of buildings. Moreover, the total energy exchanged by the buildings with the atmosphere ($Q_{ex,B}$) can be larger than just the anthropogenic sources in buildings ($Q_{F,B} + Q_{F,M}$) because it also includes the short-wave and long-wave radiation

* Correspondence to: M. Iamarino, Dipartimento di Ingegneria e Fisica dell'Ambiente, Università degli Studi della Basilicata, via dell'Ateneo Lucano 10, 85100 Potenza, Italy.
E-mail: mario.iamarino@unibas.it

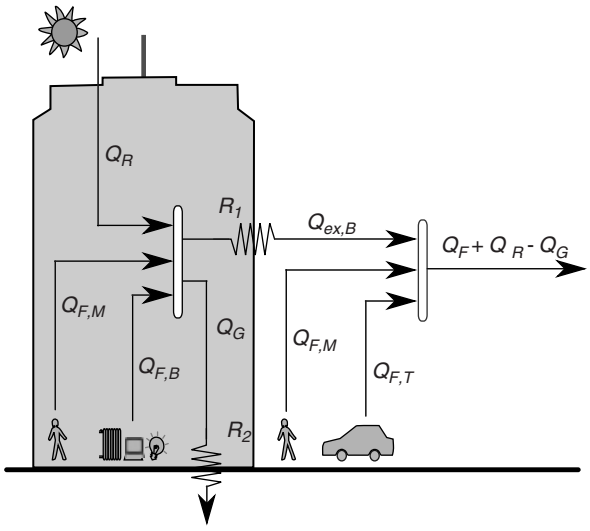

Figure 1. Anthropogenic heat and environmental loads. See text for symbol definitions.

absorbed by buildings (Q_R) less the heat dissipated into the ground (Q_G). Because of this, $Q_{ex,B}$ is not equivalent to $Q_{F,B}$ and is not defined here as the 'anthropogenic' heat flux.

Estimates of Q_F for large cities within industrialized countries mostly lie within the range of 5–100 W m^{-2} (Taha, 1997; Sailor and Lu, 2004; Allen *et al.*, 2010). Inconsistencies among the proposed values may arise from the spatial domain considered (inclusion of residential suburbs and green areas lowers Q_F), the period of the observation, the heat sources to be accounted for. Moreover, when variability is added to the analysis, results will strongly depend on the particular spatial and/or temporal resolution adopted. In general, values exceeding this range are found during daytime in central areas with tall buildings for the service industry. To accurately describe this variability, high spatial and temporal resolution is required.

For the megacity of London, the few published studies are, for different reasons, not exhaustive on this subject. One of the first studies (Harrison *et al.*, 1984) estimated an average total heat emission of 11 W m^{-2} from buildings and road traffic, with a seasonal peak of 13.8 W m^{-2} in December and a spatial range of 0–333 W m^{-2} based on a 1 km^2 grid. These values for 1971–1976 are now outdated and rely on less-accurate information on energy consumption than available at present. More recently (Hamilton *et al.*, 2009), a value of approximately 9 W m^{-2} was proposed for 2005 (spatial variability: 0–150 W m^{-2}; 1 km^2 grid), but this is limited to the building sector. The authors highlight that London $Q_{F,B}$ in winter is comparable with, and in the densely built-up areas many times larger than, the captured short-wave solar radiation, suggesting important implications to the local surface energy budget. The global model LUCY (Allen *et al.*, 2010) provided annual estimates of approximately 20 W m^{-2} for London. This does account for buildings, road traffic and metabolism but lacks the spatial resolution to extract detailed emission profiles within Greater London. Finally, none of the aforementioned studies deals with the partitioning of heat into sensible and latent fractions.

The present work aims to fill some of the gaps of earlier studies and to provide an updated and comprehensive view of the anthropogenic heat emissions across Greater London. The time period of most interest is 2005–2008, but this is considered in the context of long-term trends (1970–2025). For each source, both sensible and latent heat emissions are considered. Additionally, the heat dissipated by the wastewater collecting system (which represents a fraction of Q_G, Figure 1) is estimated. The numbers provided here are intended at the points of generation ($Q_{F,B}$ inside buildings, $Q_{F,T}$ along roads and $Q_{F,M}$ as the sum of metabolic heat emitted inside and outside of buildings, as in Figure 1) and Q_F merely is their sum. For the building sector, the actual net heat flux $Q_{ex,B}$ (Figure 1) emitted into the atmosphere was not estimated as it also requires determination of Q_R and Q_G plus the complex mechanisms of heat exchange between buildings and atmosphere (which are a combination of radiative, sensible and latent heat fluxes). These can only be addressed by an advanced building energy modelling approach, which is not among the goals of the present work. The only exception is the latent heat component of $Q_{ex,B}$ in buildings served by evaporative cooling towers, which will be briefly addressed in Section 3.3. The model developed has high spatial (200 × 200 m^2) and temporal resolution (30 min). This allows for realistic values to be determined at all times of the year at a scale that is applicable for modelling and interpreting observational data, which have changing footprint areas of this scale. To ensure the greatest flexibility of use, software is made available from which a wide range of formats, types, and ranges of output data can be chosen. The methodology could be easily exported to other urban areas in the UK and serve as a basis for cities in other countries.

The main objective of this work is to provide accurate Q_F benchmark data for different applications including urban energy balance models to assess the implication of Q_F on the urban climate, building energy models to characterize buildings-to-atmosphere/soil/water heat exchange pathways, decision support systems for urban sustainable planning, and mapping of pollutant emissions related to energy consumption in urban areas.

2. Model

Data used in this work were collected from the sources given in Table I and are referred to in the text by the acronyms listed.

The spatial domain considered here is the entire administrative area of Greater London, with a surface of 1596 km^2 and a resident population of 7 620 000 (mid-2008 estimate). Using the neighborhood statistics (NeSS) geographical hierarchy (ONS/1, Table I), Greater London can be subdivided into 33 local authorities (LA), 983

Table I. Data sources used in the present study.

Source		Description	Web link	Last retrieved
DECC (Department of Energy and Climate Change)	1	Greater London gas, electricity and other fuel consumption	http://www.decc.gov.uk/en/content/cms/statistics/regional/regional.aspx	06 August 2010
	2	History of UK energy demand (1970–2009)	http://www.decc.gov.uk/publications/basket.aspx?filetype=4&filepath=Statistics%2fpublications%2fecuk%2f266-ecuk-overall-2010.xls	06 August 2010
	3	Calorific values of UK fuels	http://www.decc.gov.uk/en/content/cms/statistics/source/cv/cv.aspx	04 October 2010
	4	Projections of UK energy demand (2010–2025)	http://www.decc.gov.uk/en/content/cms/statistics/projections/projections.aspx	04 October 2010
	5	Low carbon transition plan	http://www.decc.gov.uk/en/content/cms/what_we_do/lc_uk/lc_trans_plan/lc_trans_plan.aspx	04 October 2010
DEFRA (Department for the Environment, Food and Rural Affairs)	1	Hourly traffic data – method document	http://www.airquality.co.uk/reports/cat05/1004010934_MeasurementvsEmissionsTrends.pdf	09 November 2010
DfT (Department for Transport)	1	Manual classified count and automatic count data	http://www.dft.gov.uk/matrix/	09 November 2010
ERC (UK Energy Research Center)	1	Buildings energy load profiles	http://data.ukedc.rl.ac.uk/browse/edc	06 August 2010
GLA (Greater London Authority)	1	LEGGI 2008	http://data.london.gov.uk/datastore/package/leggi-2008-database	09 November 2010
	2	LAEI 2008	http://data.london.gov.uk/laei-2008	09 November 2010
	3	Central activities zone boundaries (London plan)	http://data.london.gov.uk/datastore/package/central-activities-zone-boundary-london-plan-consultation-2009	22 November 2010
	4	Projections of workplace and resident population in the City of London	http://www.london.gov.uk/who-runs-london/mayor/publications/business-and-economy/employment-projections-2031	26 November 2010
NG (National Grid plc)	1	UK daily gas demand	http://marketinformation.natgrid.co.uk/gas/DataItemExplorer.aspx	06 August 2010
	2	UK half-hourly electricity demand	http://www.nationalgrid.com/uk/Electricity/Data/Demand+Data/	06 August 2010
ONS (Office for National Statistics)	1	NeSS hierarchy	http://www.neighbourhood.statistics.gov.uk/HTMLDocs/downloads/NeSS_Data_Exchange_Hierarchy_Diagrams_v0.1.pdf	09 August 2010
	2	Residents, workplace and daytime population – UK 2001 National Census	http://neighbourhood.statistics.gov.uk/dissemination/	01 July 2010
	3	Time use survey 2005	http://www.statistics.gov.uk/cci/article.asp?id=160	09 August 2010

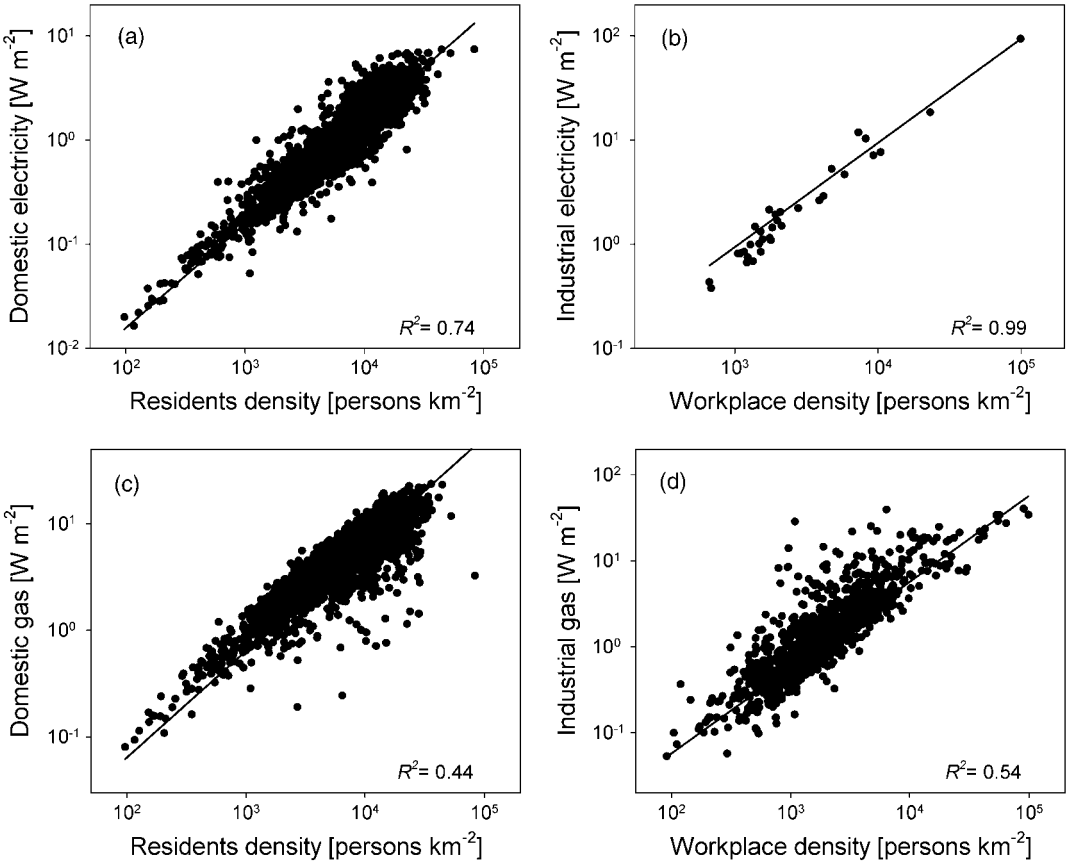

Figure 2. Annual energy consumption by sector and population density (resident or workplace): (a) domestic electricity (ordinary) at LLSOA level; (b) industrial electricity at LA level; (c) domestic gas at LLSOA level; (d) industrial gas at MLSOA level. R^2 values refer to regression of data by direct proportionality law (continuous lines). Reference year: 2008.

middle level super output areas (MLSOA), 4765 lower level super output areas (LLSOA) and 24 410 output areas (OA). The NeSS hierarchy is adopted here as a great variety of census and energy consumption data use the same spatial units.

As the NeSS units have comparable total population, they provide more detailed description in densely populated areas, although lacking accuracy in lower population density zones. Hence, a grid 200×200 m^2 is used for a more homogeneous spatial representation of results.

2.1. Buildings

Estimates of $Q_{F,B}$ are provided under the assumption that all energy consumed in buildings is released into the environment after use. The UK Department of Energy and Climate Change (DECC) publishes annual metered data of electricity (ordinary domestic, domestic Economy 7 and industrial) and gas (domestic and industrial) consumed in London during 2005–2008 (DECC/1, Table I). Industrial consumers of gas and electricity are intended as large consumers in the service and manufacturing industry, whereas Economy 7 domestic electricity is cheaper off-peak consumption at night. Annual consumption data for other fuels (non-transport petroleum, coal, manufactured fuels, renewables and waste) are available until 2007 and, in the present work, 2007 data are used for 2008 as well. DECC data have different spatial resolution. Domestic electricity and domestic gas are available at LLSOA level for 2008 and MLSOA for 2005–2007 (unallocated fraction is about 0.1% of total and is neglected). Industrial electricity is only partly allocated at MLSOA level because of the large unallocated fraction (on average, 64% in each LA) to preserve the identity of large customers. As a consequence, LA data are used instead. Industrial gas consumption is adequately allocated at MLSOA level (the unallocated fraction is $<1\%$), and consumption of other fuels is only available at LA level.

Starting from the DECC partial allocation, we disaggregate the energy consumption down to OA level. First the MLSOA domestic electricity and gas data for 2005–2007 is allocated to LLSOA in the same proportion as for 2008. Further allocation is based on the premise that domestic consumption for an area is correlated with its resident population, whereas industrial energy consumption is correlated with the amount of people who work in the area (workplace population). This assumption is confirmed in Figure 2 for domestic ordinary and industrial electricity and for domestic and industrial gas at the highest resolution available for each dataset. Here resident and workplace population refer to 2001 UK Census (ONS/2, Table I); population updates for 2005–2008 are not used as they are only for resident population and are not available below MLSOA level.

The correlations are approximately linear with R^2 values that are lower for gas than electricity and smaller spatial units. Results shown in Figure 2 provide the basis for the allocation of energy into subareas in proportion to their resident (domestic energy) and workplace (industrial energy) population fraction. Economy 7 domestic electricity and other fuels do not show a simple relation with either residents or workplace population (not shown). However, expediency suggests first scaling based on resident population, analogous to ordinary domestic electricity, and second according to a weighted average of resident (0.6) and workplace (0.4) population ($R^2 = 0.32$). The allocation of these two contributions remains very uncertain but, in combination, they account for a rather small fraction (6%) of total building energy.

Following Hamilton *et al*. (2009), daily data on UK electricity and gas demand are used to describe the temporal variability of $Q_{\mathrm{F,B}}$. These, provided by the UK utility company National Grid plc for the years 2005–2008 (NG/1 and NG/2, Table I), are for the entire UK and describe temporal trends (seasonal and weekly cycles, weather effects, holidays, etc.) that also apply to Greater London. These profiles are used to calculate daily fractions f_{d} of total electricity and gas usage in each area relative to its annual total (for other fuels, gas profile is applied). This generates aggregated daily values of domestic (E_{d}) plus industrial (E_{i}) electricity (or gas) consumption:

$$(E_{\mathrm{d}} + E_{\mathrm{i}})_{\mathrm{daily}} = f_{\mathrm{d}}(E_{\mathrm{d}} + E_{\mathrm{i}})_{\mathrm{annual}} \tag{2}$$

The partition into domestic and industrial components varies during the week and is accomplished by introducing a day of week correction factor $\lambda_{\mathrm{d},j}$ (j = working days, Saturday, Sunday) defined as:

$$\left(\frac{E_{\mathrm{d}}}{E_{\mathrm{i}}}\right)_{\mathrm{daily}} = \lambda_{\mathrm{d},j}\left(\frac{E_{\mathrm{d}}}{E_{\mathrm{i}}}\right)_{\mathrm{annual}} \tag{3}$$

The $\lambda_{\mathrm{d},j}$ are computed from the daily variations of $E_{\mathrm{d}}/E_{\mathrm{i}}$ in the 30-min Energy Research Center (ERC) energy load reference profiles (ERC/1, Table I) for domestic and industrial electricity consumers for weekdays, Saturday and Sunday and for five times of year: autumn, winter, spring, summer and high summer. These are $\lambda_{\mathrm{d},1} = 0.79$ (working days), $\lambda_{\mathrm{d},2} = 1.11$ (Saturdays) and $\lambda_{\mathrm{d},3} = 1.78$ (Sundays plus bank holidays), with no significant seasonal variation. Finally, for every day of the year, the daily domestic and industrial electricity (or gas) is obtained by solving Equations (2) and (3) simultaneously.

ERC profiles are also the basis for the 30-min profiles starting from the daily amounts. For this, the domestic gas load profile is assumed equal to domestic unrestricted electricity and industrial gas and other fuels load profiles are assumed equal to non-domestic electricity.

2.2. Transportation

Here road traffic is considered but other modes of transport in London, e.g. trains (overground and underground) and ships (expected to be small), are not considered. For trains, which are mostly electric (some diesel), the braking mechanism determines whether waste heat is lost or recovered.

For road transportation the methods used to determine $Q_{\mathrm{F,T}}$ follow the London Greenhouse Gas Inventory (LEGGI 2008; GLA/1, Table I) and the London Atmospheric Emissions Inventory (LAEI 2008; GLA/2, Table I). The hourly estimates of total vehicle fuel use F (g km^{-1}) for a year (t) and by fuel type (j) are determined by the numbers of each of 11 different vehicle types (i), based upon annual average daily total (AADT) traffic, travelling at a speed (S), age profile (a), split by Euro class, for each year and the emission rate (β) for each vehicle type and Euro class combination.

$$F_{j,\mathrm{t}} = \sum_{i=1}^{11} V_{i,\mathrm{j}}\ a_{i,j,\mathrm{t}}\ \beta_{i,j,\mathrm{t,s}} \tag{4}$$

The AADT estimates include both weekend and seasonal effects. Each of the approximately 6500 road links (length D_{k}) are classified based on how the traffic counts are determined: (1) Major (roads with regular count data), (2) LTS (smaller roads, using traffic model estimates of flow and speed) and (3) Minor (residual from Transport for London (TfL) annual total estimates after Major and LTS are accounted for) and distributed across London based on length of minor roads in each km^2. The fuel use (F) is combined with the heat of combustion C for two fuel types (j), i.e. gasoline and diesel (Table II):

$$Q_{\mathrm{F,T_{k,t}}} = D_{\mathrm{k}} \sum_{i=1}^{2} F_{j,\mathrm{t}} C_j \tag{5}$$

For 2008, these calculations were expanded to give hourly estimates of $Q_{\mathrm{F,T}}$ for any road or group of roads chosen in London. This required the development of an hourly traffic file, calculated using a 'London averaged' automatic traffic counts (ATC) from sites in central London, running between 2003 and 2008 (Department for the Environment, Food and Rural Affairs/1, Table I). To avoid the problem of introducing an artificial trend into the hourly data using the London averaged counts, a generalized additive modelling (GAM) technique was applied to the dataset, using similar methods to Carslaw *et al*. (2007). GAM modelling established that hourly

Table II. Gross and net heat of combustion UK fuels (DECC/3, Table I).

	Heat of combustion (MJ kg^{-1})	
	Net	Gross
Natural gas	35.5	39.4
Petrol fuel	44.7	47.1
Diesel fuel	43.3	45.5
Crude oil	43.4	45.7

Table III. Data used to calculate the average metabolic rate (see text for details).

Age	0–4	5–14	15–19	20–24	25–44	45–59	60–79	≥80	
P (*persons*)	478 800	888 700	418 500	542 800	264 8000	116 4900	939 900	240 700	
Activity (or equivalent)					*t* (h)				*M* (W m^{-2})
Sleeping	13.0	10.0	9.0	8.5	8.0	8.0	8.5	9.0	40
Sitting, at rest	3.0	2.0	1.0	0.5	0.5	1.0	2.5	7.0	55
Standing, at rest	1.0	1.0	0.5	0.5	0.5	0.5	1.0	1.0	70
Sitting, light activity	3.0	4.0	4.5	5.0	5.0	5.0	4.5	4.5	70
Standing, light activity	2.0	3.5	3.0	3.0	3.5	3.0	3.0	1.0	93
Standing, medium activity	1.0	2.0	2.0	2.5	2.0	2.0	2.0	0.5	116
Walking on the level	1.0	1.0	2.0	2.0	2.0	1.5	1.5	1.0	140
Walking uphill, ladder, etc.	0.0	0.5	1.0	1.0	1.0	1.0	0.5	0.0	200
Hard work	0.0	0.0	0.5	0.5	1.0	1.0	0.5	0.0	230
Very hard work, sport	0.0	0.0	0.5	0.5	0.5	0.5	0.0	0.0	290
f_R (−)	1.31	1.10	1.08	1.03	1.00	0.97	0.92	0.89	
A (m^2)	0.5	1.07	1.5	1.7	1.8	1.8	1.75	1.7	

traffic counts could be described using smooth functions of hour of day, day of week, season and trend. On average, these factors could account for R^2 approximately 0.9 of the hourly values. The analysis found no significant long-term trend in the hourly data.

To calculate hourly total traffic flows, road by road, the 'London averaged' data were scaled using manual classified count (MCC) data taken during weekday periods (7 : 00–19 : 00). Unlike the ATC data, manual counts are widespread and cover all of the major roads in London. However, manual count data are infrequent and may be highly variable because of specific local events; the MCC time series for each major road were smoothed using local regression (Jacoby, 2000). When few measurements (<3) were available, an average for the road was used. Daytime, night-time, weekday and weekend differences in vehicle flow are accounted for.

The MCC data, for the 11 vehicle types, were used to split the total vehicle count for each hour of the day. As less data are available for nocturnal weekdays, Saturdays and Sundays the 24 h MCC data were combined with the automatic number plate recognition camera data (TfL, personal communication), which gives highly time resolved (1 s) vehicle data at 30 sites in London.

The total hourly vehicle counts summarized by the time of day and the day of week for 2008 are compared with Department for Transport ATC data (DfT/1, Table I and personal communication) for 2006 and 2007 and not used in the model development. Comparison over 16 site years shows that very little bias exists in the predictions (in all cases below 7%). Lack of data during weekends is apparent with the poorest performance on Saturdays. However, Sunday is well predicted and for the entire 2 year period an average root mean square error of approximately ±10% existed between the predicted and measured traffic data. This provided a robust hourly traffic dataset from 2003 to 2008, from which 2008 was chosen for the $Q_{F,T}$ calculations.

The annual average values of $Q_{F,T}$ for each 1 km^2 grid by road type (Major, LTS and Minor) for each year (2005–2008) are proportionally distributed into the 200 × 200 m^2 grid by road length. The annual data are distributed into hourly profiles based on 2008 profiles, which are linearly interpolated to obtain 30-min resolution. The 2008 hourly profiles are available for each major road by vehicle type for a typical week (generic Monday to Sunday, one profile for each; Sunday profile applied to holidays). Here one average 30-min profile for each vehicle type for entire London is used, regardless of road.

2.3. Human metabolism

The heat flux $Q_{F,M}$ generated by the human metabolism in a generic area is computed as:

$$Q_{F,M} = r(t)\,p(t) \tag{6}$$

where $r(t)$ is the time-dependent average metabolic rate (W person^{-1}) and $p(t)$ is the population time profile in the area considered.

To calculate $r(t)$ the following data are considered (Table III): London resident population P by eight age groups (ONS/2, Table I); time t spent by each group in different activities (ten classes), redistributed from the UK Time Use Survey 2006 (ONS/3, Table I); standard metabolic rates M (W m^{-2} of body surface area) of a standard person (30 years old, average body) for each activity (ISO 8996, 2004); age correction factors f_R to account for variation of M with age (Altman and Dittmer, 1968) and mean body surface area A for each age group (Mosteller, 1987). f_R and A are calculated as average for males and females by assuming a 1 : 1 male-to-female ratio.

The metabolic rates r_N at night (sleeping) and r_D during daytime (remaining activities) are:

$$r_N = M_1 \sum_{j=1}^{8} \left(f_{R,j} A_j \frac{P_j}{P_{tot}} \right) = 64.3 \text{ W} \tag{7}$$

$$r_{\mathrm{D}} = \sum_{j=1}^{8}\left(f_{\mathrm{R},j}\,A_j\,\frac{P_j}{P_{\mathrm{tot}}}\sum_{i=2}^{10}\left(\frac{t_{ji}}{24-t_{1i}}M_i\right)\right) = 170.5\ \mathrm{W} \tag{8}$$

where index j refers to the eight age groups, index i covers the ten specific activities ($i = 1$ for sleeping). The values computed in Equations (7) and (8) are similar to values adopted in previous studies: Sailor and Lu (2004) used 75 and 175 W and Smith *et al.* (2009) used 70 and 250 W. Finally, $r(t)$ is given by r_{N} between 0 : 00 and 6 : 00 and by r_{D} between 9 : 00 and 21 : 00, whereas an arbitrary smoothed connection function has been imposed between 6 : 00 and 9 : 00 and between 21 : 00 and 0 : 00 (Sailor and Lu, 2004).

The time profile $p(t)$ used for the effective population in a certain area is a consequence of the daily fluxes of people entering/leaving the area when reaching/leaving their place of work. It is based on the resident and daytime population for an area. The latter is defined as 16–74 year olds who live and work in the area (or do not work) plus those who live outside the area but work in the area (ONS/2, Table I). On work days, $p(t)$ is given by residents between 20 : 00 and 7 : 00 and by daytime population from 10 : 00 to 16 : 00 with a smoothed connection function for the transition. On Saturday, Sunday and bank holidays, only residents are considered in each area; for some shopping areas this may result in some under counting.

2.4. Partitioning of Q_{F}

The components of Q_{F} (Sections 2.1–2.3) are total heat, which can be partitioned into (atmospheric) sensible and latent fraction and into wastewater heat.

For fossil fuels combustion, sensible heat is calculated by multiplying the corresponding total Q_{F} by the net-to-gross heating value ratio of the fuel (Table II). For combustion of other fuels, the heating value of crude oil is used because petroleum products represent more than 90% in this group. The latent heat flux is the difference (total - sensible heat) and represents the energy stored in the water vapour generated by reaction, when the reaction products are cooled to ambient temperature with respect to liquid water at the same temperature. Data on the impact of condensing boilers were not available so they are not considered; this will result in an overestimate of latent heat associated with some stationary sources. It must be noted that some authors (Sailor, 2011) do not include the latent heat from combustion processes in the anthropogenic latent heat emissions, based on the argument that chemical reactions do not involve a tangible phase change.

For electricity, the total heat flux from electricity consumption is assumed to be entirely released in the form of sensible heat.

For metabolism, the latent heat fraction depends on ambient conditions and activity and goes from about 20% of $Q_{\mathrm{F,B}}$ during sitting and resting up to 60% and more during intense physical activity (Jones, 2001). Here, a constant average fraction of 30%, typical for office work, is considered.

A heat-to-wastewater flux is computed by considering the sensible energy used to heat water. For the domestic sector, this is 13.9% of total electricity and 27.0% of total gas, and, for the industrial sector, 3.6% of total electricity, 14.6% of total gas and 8.4% of other fuels (DECC/2, Table I). By multiplying these quantities by the typical efficiency of electrical heaters (0.98) and fired heaters (0.85), the fractions of sensible energy transferred to hot water are obtained. Here it is assumed this energy is entirely removed by the underground wastewater collecting system, i.e. heat exchange between hot water and building is neglected.

Heat emissions from cooling systems and, in particular, latent heat emissions from evaporative cooling towers and evaporative condensers used in large centralized cooling equipments have received attention recently (Moriwaki *et al.*, 2008). Cooling towers reject heat from the internal building volume (lowering the building-to-atmosphere heat transfer resistance R_1, Figure 1) by evaporating water (i.e. turning sensible heat into latent heat) that is then released into the atmosphere, whereas air cooled systems perform a similar operation but eject sensible heat. This energy is a combination of heat dissipated from appliances, lights, humans, etc. located in the building (all of anthropogenic nature) and solar gain of the building (of non-anthropogenic nature, according to definitions used here, see Equation (1)). As the anthropogenic terms are already accounted for in $Q_{\mathrm{F,B}}$ and $Q_{\mathrm{F,M}}$ together with the energy required to run the cooling system, the presence of cooling devices does not call for any special intervention on the model developed here. Nevertheless, because of their potential important role in some areas, a brief account is given (Section 3.3) of the additional emissions of latent heat produced by evaporative cooling systems.

2.5. The software GreaterQF

To ease computing and visualization of spatial and temporal profiles of Q_{F} in Greater London, the software GreaterQF (version 3.2) has been developed and made available (http://geography.kcl.ac.uk/micromet/). It is an executable Microsoft Windows application built within the development environment Embarcadero Delphi® XE. During a preprocessing stage, external data are imported, disaggregated and allocated onto the common operational level termed as SubOA, given by the intersection of the NeSS areas with the 200×200 m^2 grid. From the 147315 SubOAs, all other spatial units can be generated.

Results can be obtained as total Q_{F} or fraction (sensible, latent and heat-to-wastewater), individually for all sources considered in this work, with the desired spatial resolution (200×200 m^2 grid or any of the NeSS units) and temporal resolution (30 min–1 year). Output is graphical or as a textfile suitable for geographic information system analysis or for import to other models.

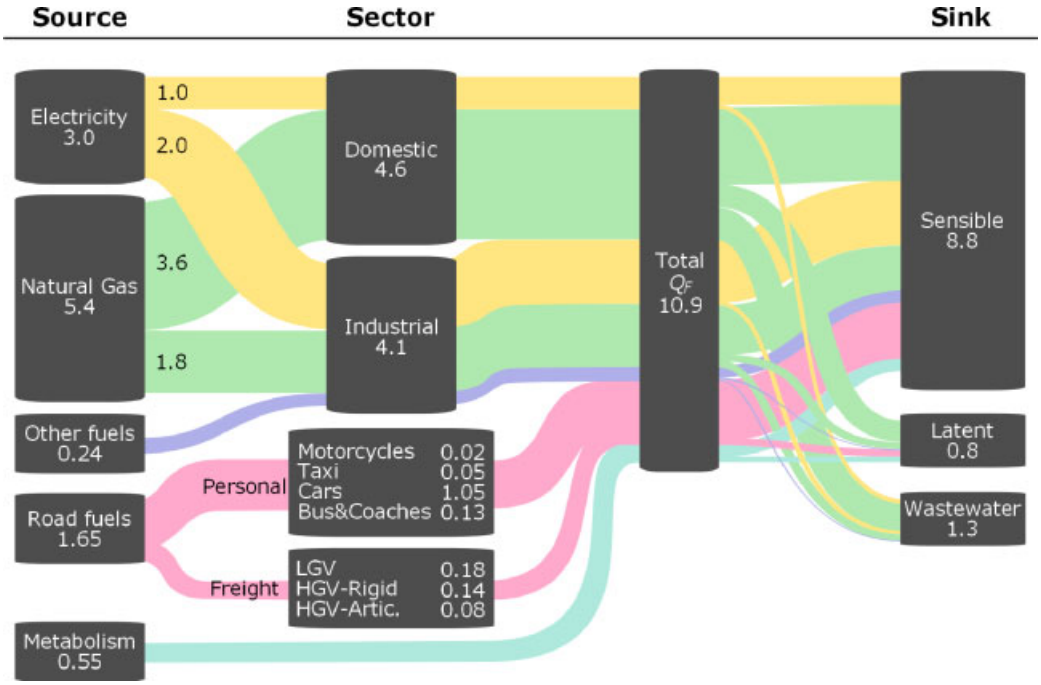

Figure 3. Q_F (W m^{-2}) over Greater London by source, sector and sink (2005–2008). This figure is available in colour online at wileyonlinelibrary.com/journal/joc

3. Results and discussion

For the years 2005–2008, the average total anthropogenic flux over Greater London was 10.9 W m^{-2}. Energy flows classified by source, sector and sink are shown in Figure 3. The largest contribution is from the building sector as a whole, 8.7 W m^{-2} (80% of total, of which 42% is domestic and 38% industrial). This is followed by the transportation sector, which contributes 1.65 W m^{-2} (15%), where cars are by far the most important source of heat emissions (accounting for 64% of the transportation sector and 10% of total Q_F), followed by light goods vehicles, rigid heavy goods vehicles (HGVs) and buses and coaches. The impact of taxi, motorcycles and articulated HGVs is negligible (all <0.1 W m^{-2}). Finally, human metabolism contributes 0.55 W m^{-2} (5.1%). As concerns the sinks, the largest fraction of total Q_F is emitted as sensible heat to atmosphere (8.8 W m^{-2}, 81% of total), while only small fractions are emitted as latent heat through the release of water vapour (0.79 W m^{-2}, 7.3%) or lost in the wastewater system (1.3 W m^{-2}, 12%).

The average fluxes in Figure 3 appear modest, but all together they correspond to 150 TWh annually released into the environment in Greater London. Moreover, these fluxes are very unevenly distributed in time and space with peaks up to orders of magnitude greater than the average values, as addressed in the next two sections.

3.1. Spatial variability

The spatial variability of Q_F by sector is shown in Figure 4 with 200 × 200 m^2 resolution. The domestic heat emissions (Figure 4(a)) appear rather homogeneously distributed in space, with peak values up to 36.5 W m^{-2}, whereas industrial (all non-residential buildings) emissions (Figure 4(b)) are very concentrated in Central London (peaks up to 197 W m^{-2}). Emissions from road traffic (Figure 4(c)) follow, as expected, the London road network and the routes of major roads are easily identifiable. In some cells with major road junctions, peak emissions are up to 48 W m^{-2}. Metabolic heat emissions (Figure 4(d)) have a spatial distribution similar to industrial energy with higher values in central areas (peaks up to 6.4 W m^{-2}), where people are more concentrated in the daytime. The resulting total Q_F (Figure 4(e)) cumulative distribution function (Figure 4(f)) has been folded to highlight its positive skewness as evidenced by the long tail on the right of the median value, 8.0 W m^{-2}. It follows that 50% of London surface experiences annual total heat emissions less than 8.0 W m^{-2} and only 2.5% has values greater than 50 W m^{-2}. Most of these high values fall within a restricted area of Central London defined in the London plan of the Greater London Authority (GLA/3, Table I) as the central activities zone (CAZ, indicated with dashed boundaries in Figure 4(e)). The CAZ surface (33.5 km^2) is just 2% of Greater London, but it accounts for one third of the total industrial energy consumption because of the very high concentration of service industry (government offices and other institutions, financial and business services, large shopping quarters, extensive activities associated with tourism, entertainment, education, communication, etc).

The greatest emissions in the CAZ are within the City of London, the smallest London borough (3.2 km^2, continuous boundaries in Figure 4(e)). This area contains some of the largest and most high-standard office buildings in London where a very large number of people

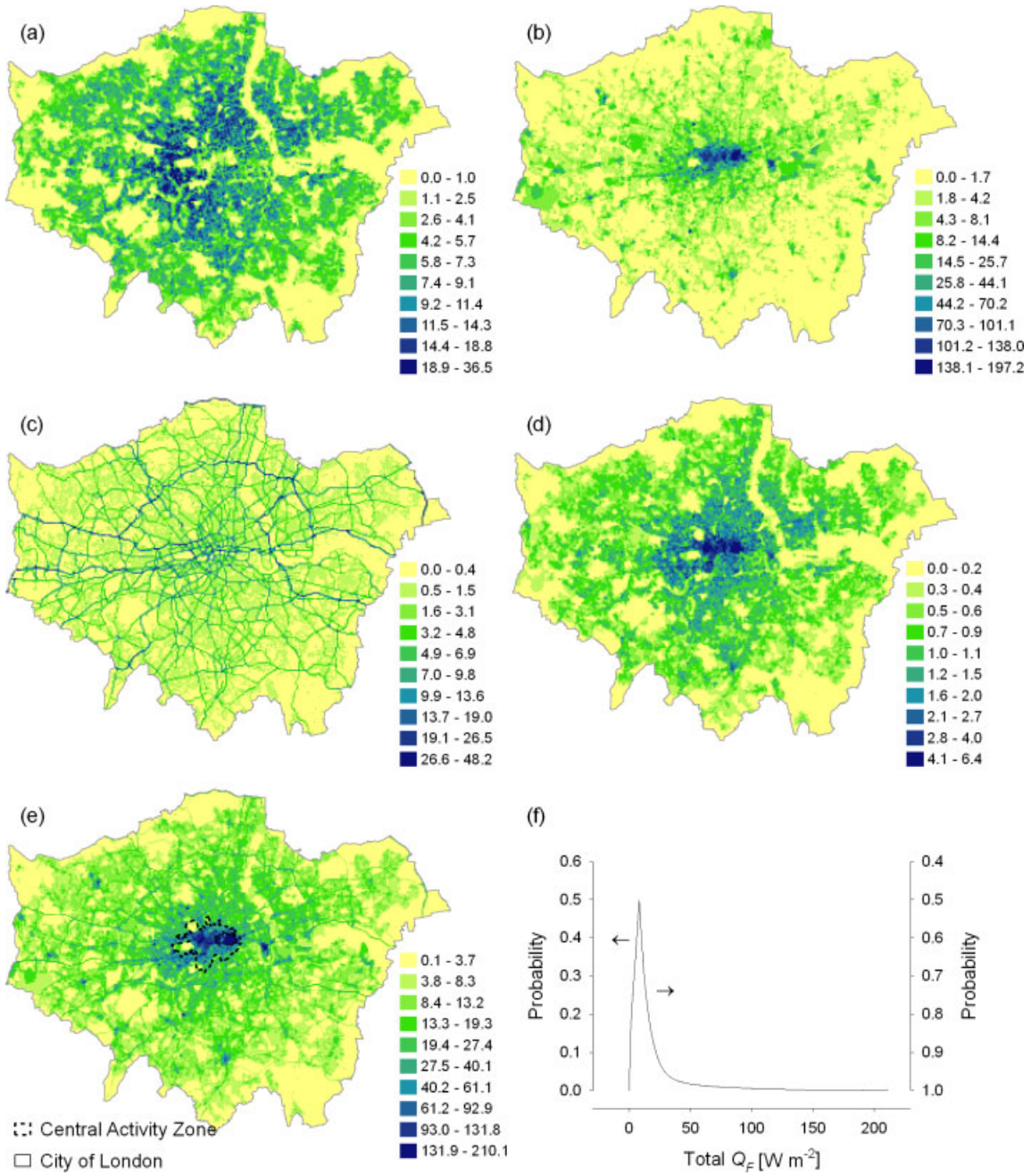

Figure 4. Spatial variability of heat emissions (average for 2005–2008) at 200 × 200 m^2 resolution by sector: (a) domestic, (b) industrial, (c) road traffic, (d) metabolism and (e) total (classes by Jenks natural breaks) and (f) folded cumulative distribution function of total Q_F (f). Values in W m^{-2}. This figure is available in colour online at wileyonlinelibrary.com/journal/joc

work (348 000 people in 2007). The average Q_F is 140 W m^{-2} with local peaks up to 210 W m^{-2}. Other extreme values within the CAZ can be found along the axis Oxford Street – Regents Street – Piccadilly Circus (values up to 146 W m^{-2}), along Victoria Street (160 W m^{-2}), around Euston Square (181 W m^{-2}) and Knightsbridge (143 W m^{-2}). Outside the CAZ, it is worth noting the 145 W m^{-2} in the Canary Wharf area located a few kilometers eastwards: heat emissions in this business and financial district, which hosts the three tallest skyscrapers in the UK, is expected to grow in the future because of the completion of more large office buildings.

For practical or predictive purposes, a first order estimate of the total heat released by buildings (domestic + industrial) in an area is given by:

$$Q_{F,B} = k d_c \tag{9}$$

where k is a proportionality constant, d_c (persons m^{-2}) is a corrected population density calculated as weighted average (of weight w) of the workplace (d_w) and resident (d_r) population density of the given area:

$$d_c = w d_w + (1 - w) d_r \tag{10}$$

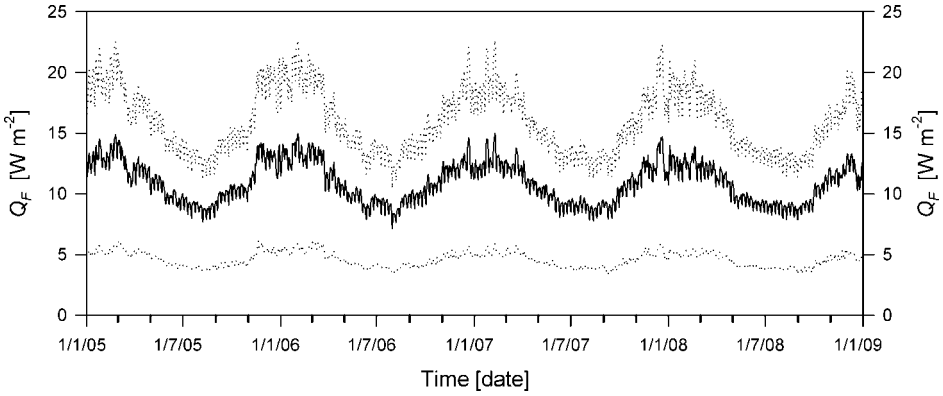

Figure 5. Temporal variation (2005–2008) of total Q_F for Greater London as average (solid) and minimum/maximum (dotted lines) daily values.

This type of correlation directly follows from the use of resident and workplace population densities to scale energy consumption in buildings. The best fit for entire Greater London is obtained when $k = 2160$ W person^{-1} and $w = 0.58$ ($R^2 = 0.92$); evidently, this also corresponds to using a constant heat emission factor per resident population, $k(1-w) = 907$ W person^{-1}, and a constant heat emission factor per workplace population, $kw = 1253$ W person^{-1}. A similar empirical relation cannot be given for $Q_{F,T}$ because road traffic cannot be easily correlated with population, land-use or other indicators.

3.2. Temporal variability

From the daily Q_F average values and daily minimum/maximum range (Figure 5) for 2005–2008, the seasonal variability is clear, with higher values in winter because of increased energy load for space heating. Moreover, there is no clear evidence of summer energy consumption peaks (e.g. because of air conditioning) as it is typical in warmer climates (Psiloglou *et al.*, 2007). The maximum relative deviation of winter Q_F with respect to summer is around 80%, which is much less than predicted at London's latitude (51°N) (Ferreira *et al.*, 2010). This can be explained partly by London's climate that has smaller temperature fluctuations between summer and winter compared with continental cities at similar latitude. Overall, there is a small negative trend in Q_F during the 4 years, which is only slightly perceivable on Figure 5, and that will be addressed quantitatively in Section 3.4 relative to longer term trends.

The daily minima (usually between 2:00 and 5:00) have a smaller seasonal oscillation compared with the range in the maxima (reached between 12:00 and 19:00 depending on season and day of week).The 24-h range has a mean of 15 W m^{-2} in winter and 7 W m^{-2} in summer. However, for some grid cells in the CAZ, the difference is up to 300 W m^{-2} in winter.

Examples of the half-hourly profiles for a typical week in January 2008 (Monday 14 to Sunday 20) are shown in Figure 6 for two representative grid cells: cell ID 22030 in the City of London with predominant emissions from the service industry and ID 22642 in a residential neighborhood in Southwark with predominant emissions from the domestic sector. In both, the residential emission profile on working days has two peaks (Figure 6(a)), a lower one in the morning (between 8:00 and 9:00) and a second, higher one in the evening (18:00–19:00). This reflects the pattern of occupancy of dwellings and the corresponding energy needs. In contrast, industrial emissions peak only once between 11:00 and 12:00 (Figure 6(b)), when activities in the service industry are at their maximum. The situation is different at weekends, when industrial emissions drop and domestic emissions increases lightly. With respect to road traffic, emission profiles for personal transportation (Figure 6(c)) have two peaks on working days (at 8:00–9:00 and at 16:30–17:30) corresponding to the main movements of people to/from their workplace/schools etc. with smoother profiles during weekends. Freight transport (Figure 6(d)) emissions are also double-peaked during the week with highest values in the early morning and at around midday, with large reductions on Sunday. Emissions from human metabolism also reflect movement of people (Figure 6(e)): in the CAZ cell, metabolic emissions are extremely high during working days and fall during the night and on weekends when people are not present. While in the residential cell, the profile has the typical double peak during working days according to the presence of people at home and a plateau on weekends because of occupancy throughout the day. The lower values during the night are because of the reduced metabolic rates (Section 2.4). The total Q_F (Figure 6(f)) are consequently shaped by the predominant emitting sector (domestic and industrial buildings, respectively).

3.3. Sensible, latent and wastewater heat

Across the temporal and spatial domain considered, the Q_F partitioning does not differ significantly from the proportions in Figure 3. The sensible heat fraction occasionally can be lower in residential areas, because of the higher hot water needs (which increases the heat-to-wastewater fraction) and the greater importance of natural gas consumption (which increases the latent heat fraction). It is slightly higher in areas with consumption dominated by the service industry because of the more

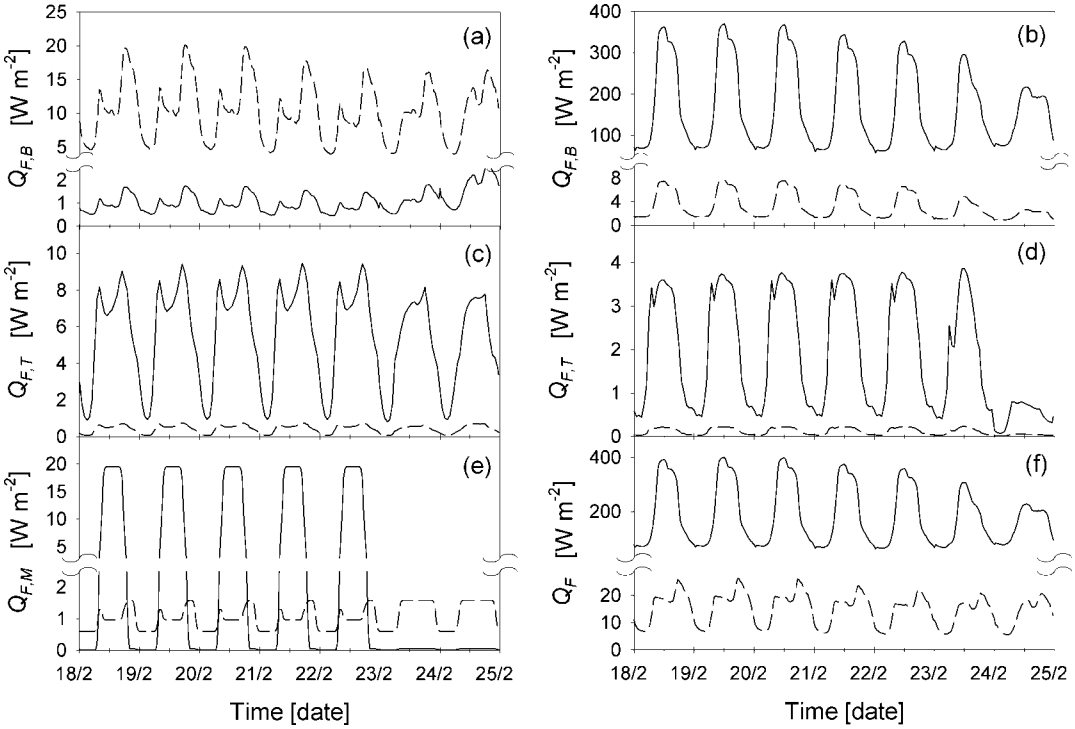

Figure 6. Half-hourly heat emissions during 18–24 February 2008 (Monday to Sunday) for cell ID 22030 (solid) and 22642 (dashed) from: buildings [(a): domestic and (b): industrial], road traffic [(c): personal and (d): freight], (e) metabolism and (f) total Q_F. Note the vertical axis is broken and different between graphs.

extensive use of electricity (which does not produce latent heat).

Apart from the anthropogenic latent heat flux determined by the present model, buildings can be the source of additional latent heat because of the presence of evaporative cooling towers often used in large air conditioned centralized systems. In London, where summers are mild, artificial cooling is almost completely absent in the domestic sector and is used only by the high-standards service industry. According to the cooling towers registers held by the London Borough Councils, more than half of the around 2000 cooling towers in operation in Greater London are concentrated within the CAZ and Canary Wharf. To assess the implications of this high concentration, the case of OA 00AAFZ0001 (0.39 km^2) within the City of London is analysed. This area has large office buildings and its business nature is evident from the contrasting workplace population (39 000 people) to the few residents (141). Seventy-seven evaporative cooling towers are in operation in this OA and serve 28 buildings, corresponding to 29% of the total OA building volume. Assuming that cooling involves the entire volume of these 28 buildings, the typical summer day profile of latent heat flux generated by the cooling towers can be estimated as:

$$Q_{\mathrm{lat,B}}(t) = (1 + COP)E_{\mathrm{c}}(t)\frac{A_{\mathrm{c}}}{A_{\mathrm{OA}}} \qquad (11)$$

where $E_{\mathrm{c}}(t)$ is the average time profile of cooling power consumption (W m^{-2}) in a UK office in summer (based on data from Knight and Dunn, 2002), COP is the coefficient of performance corresponding to the energy transferred to the outside per unit of electrical energy spent (2.0 and 4.0 are used to represent low and high efficiency cooling systems, respectively; Stanford, 2003), A_{c} is the estimated total cooled floor area ($4.1 \cdot 10^5$ m^2), and A_{OA} is the surface of the OA ($3.9 \cdot 10^5$ m^2). The resulting $Q_{\mathrm{lat,B}}$ daily profile in summer is reported in Figure 7 for both COP values. For both cases the latent heat fluxes are considerably larger than the total $Q_{\mathrm{F,B}}$ (sensible + latent) estimated for the buildings served by these cooling towers (evaluated as 29% – i.e. the same proportion as building volume of $Q_{\mathrm{F,B}}$ for the entire OA). This agrees with previous findings (Sailor *et al.*, 2007) and is because of the fact that $Q_{\mathrm{lat,B}}$ also includes a large part of the solar radiation captured by the buildings during

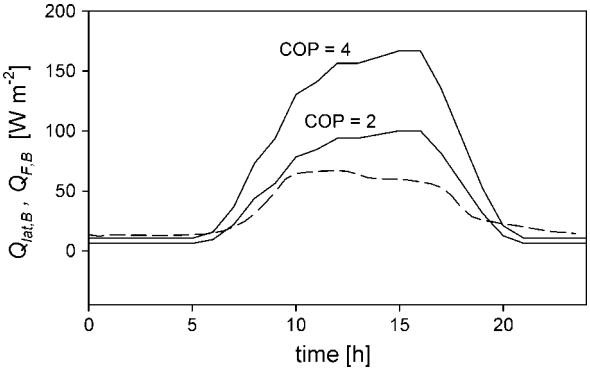

Figure 7. Summer day latent heat emissions $Q_{\mathrm{lat,B}}$ from buildings with cooling towers in output area 00AAFZ0001 at different COP (solid) and $Q_{\mathrm{F,B}}$ from same buildings (dashed).

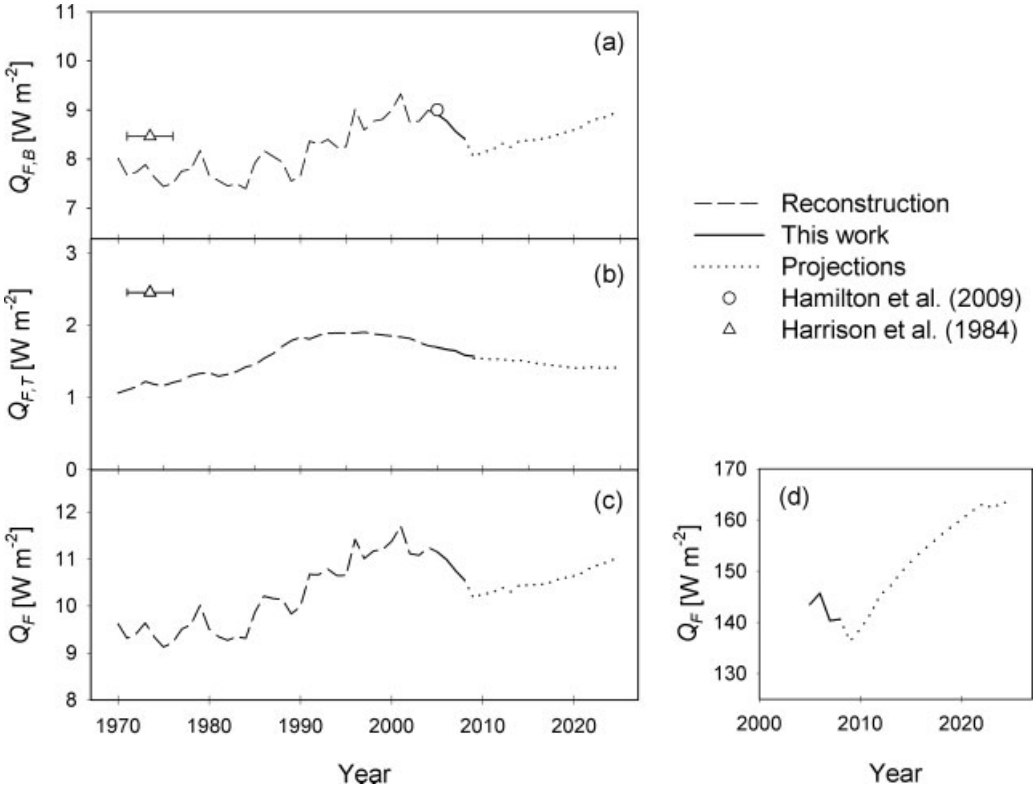

Figure 8. Heat emissions in Greater London for 1970–2025 for (a) building sector, (b) road traffic and (c) total; and (d) total emissions in the City of London for 2005–2025.

the day. Moreover, as this flux only represents the latent heat component of the total heat flux $Q_{ex,B}$ exchanged by the buildings with the atmosphere (Figure 1), this total flux is expected to be even higher and introduces the need for a more complete building modelling approach if the building-atmosphere interaction is to be described in detail.

3.4. Long-term trends

The results have been extended back to 1970 and forward until 2025. For the building sector, this is achieved by applying the same long-term trends proposed by DECC as baseline for the entire UK (DECC/2 for 1970–2004 and DECC/4 for 2009–2025, Table I). An annual correction factor has been introduced to account for differences in London population dynamics relative to the UK, based on population history and projections (ONS/2, Table I). For road traffic, reconstruction in the past is consistent with the London LAEI emissions inventory (GLA/2, Table I) and future forecasts have been provided by TfL (personal communication).

For the building sector (Figure 8(a)), $Q_{F,B}$ during 1970–1990 oscillated around 7.7 W m^{-2} as the slowly increasing UK per-capita energy consumption over this period was balanced by a decrease in London population, which reached a minimum in 1982. After that, emissions have increased and peaked in 2001 (9.3 W m^{-2}). From 2002, the gradually increasing price of fuels and, more recently, the slowing down of UK economic growth have caused a continuous decrease in energy consumption. The minimum is expected to have been reached in 2009 and a slow recovery is forecast from 2010 with a return to pre-crisis levels by 2020 (if expectations of fuel prices, national gross domestic product and population dynamics are met). Heat emissions from the transportation sector (Figure 8(b)) have been constantly increasing from 1970 until the mid-1990s, with values almost doubling during this period. The subsequent decreasing trend, which is counter to the trend of continuously increasing level of road traffic in the rest of the UK, is a result of measures undertaken by the GLA to control traffic-related pollution and is expected to continue in the coming two decades. The resulting total Q_F (Figure 8(c)), which includes metabolic $Q_{F,M}$ adjusted according to population dynamics, has a long-term trend that closely follows $Q_{F,B}$ with a maximum of 11.7 W m^{-2} in 2001 and a recent relative minimum of 10.2 W m^{-2} in 2009.

Interestingly, for the years 1971–1976, poor agreement is found with road traffic emissions of 2.5 W m^{-2} estimated over Greater London by Harrison *et al.* (1984), which is double the value suggested here (1.2 W m^{-2} mean for same years). However, estimates for the building sector are closer (8.5 *vs* 7.6 W m^{-2}). Better agreement is found with the more recent work of Hamilton *et al.* (2009) for $Q_{F,B}$ in 2005 since same DECC data for that year have been used.

The trend for the next 25 years is encouraging in that no dramatic increase of London Q_F is forecasted in the medium term. This might not be true locally, especially in the CAZ area and in its financial core City of London,

which will experience further concentration of activities in coming years. Projections of workplace population in the City of London have been recently addressed by the Greater London Authority (GLA/4, Table I) and are based on planned availability of office space, area's accessibility and employment trends. According to this analysis, 80 000 additional workers are expected by 2025 in the city, bringing to 430 000 the total number of people working in an area of just 3.2 km^2. Projections for the City of London can be made for $Q_{F,B}$ by applying Equations (9) and (10) after determination of k and w using GLA projections of d_w and d_r and by correcting for the expected national trend in domestic and industrial energy consumption. The $Q_{F,M}$ can be estimated based on expected resident and workplace population dynamics, and $Q_{F,T}$ can be projected using the overall London trend of Figure 8(b). The resulting total Q_F in the City of London is reported in Figure 8(d) and is expected to recover much faster and reach 165 W m^{-2} by 2025 (with 16% increase with respect to 2005). Analogous situations are expected in other expansion areas, in particular Canary Wharf, where the workplace population is projected to double by 2025.

Less pessimistic projections are obtained if the UK 2008 adoption of the ambitious targets of 80% reduction in greenhouse gas emissions by 2050 is taken into account. Different routes to reach this target, as the low carbon transition plan (LCTP; DECC/5, Table I), indicate a consistent need to pursue increasing energy efficiency in buildings and discourage final energy demand, hence also strongly cutting anthropogenic heat emissions in urban areas. When the LCTP scheme is considered, the average Q_F in Greater London is expected to drop to 9 W m^{-2} by 2025. However, in the City of London the LCTP scheme will be able, at best, to keep heat emissions in this area at about the same levels as in 2008.

4. Conclusions

Using the methods described, the three main contributions to Q_F in Greater London and their variability in time and space are estimated. It is concluded that buildings, the major source of anthropogenic heat emissions, account for about 80% of the nearly 150 TWh of waste energy annually emitted across the city. The method used to estimate the spatial variability of $Q_{F,B}$ is a novel top-down approach based on high-resolution resident and workplace population data. Uncertainties are unavoidably associated with this method, but the allocation errors do not propagate outside the smallest spatial units at which external energy consumption data are available for each sector.

The spatial patterns of heat emissions over the London surface are homogeneous for the domestic sources, whereas in the industrial sector, especially the service industry, they are very concentrated in restricted areas with very high peaks. As a consequence, only 2.5% of London surface experiences annual fluxes above 50 W m^{-2}. The highest emissions are in the City of London, with average values up to 210 W m^{-2} for total Q_F. When temporal variability is considered, the peak values are up to 550 W m^{-2}.

Projections to 2025 indicate a possible increase of heat emissions in areas such as the City of London because of further intensification of activities based on the expansion plans. However, the extent of such increases depends primarily on how successful efforts are in cutting greenhouse gas emissions, and hence, energy demand in the UK as committed to in the coming decades.

Acknowledgements

The contributions of Rossella Perniola (former student, University of Basilicata, Italy), Dr Fredrik Lindberg (King's College London, UK, and Gothenburg University, Sweden) and Kandarp Amin (Nuffield student, King's College London, UK) to this work are gratefully acknowledged. National Grid plc is acknowledged for providing data on UK gas and electricity demand. Charles Buckingham from Transport for London is acknowledged for providing traffic projections. Funding from the European Union Seventh Framework Programme FP/2007-2011 grant agreements 212520 (MegaPoli) and 211345 (BRIDGE) is gratefully acknowledged.

References

Allen L, Lindberg F, Grimmond CSB. 2011. Global to city scale urban anthropogenic heat flux: model and variability. *International Journal of Climatology* **31**, DOI:10.1002/joc.2210.

Altman PL, Dittmer DS. 1968. *Metabolism*. Federation of American Societies for Experimental Biology: Bethesda, Maryland.

Carslaw DC, Beevers SD, Tate JE. 2007. Modelling and assessing trends in traffic-related emissions using a generalized additive modelling approach. *Atmospheric Environment* **41**: 5289–5299, DOI:10.1016/j.atmosenv.2007.02.032.

Ferreira MJ, Oliveira AP, Soares J. 2010. Anthropogenic heat in the city of São Paulo, Brazil. *Theoretical and Applied Climatology* **104**: 43–56, DOI: 10.1007/s00704-010-0322-7.

Grimmond CSB. 1992. The suburban energy balance: methodological considerations and results for a mid-latitude west coast city under winter and spring conditions. *International Journal of Climatology* **12**: 481–497, DOI:10.1002/joc.3370120506.

Grimmond CSB, Blackett M, Best MJ, Barlow J, Baik JJ, Belcher SE, Bohnenstengel SI, Calmet I, Chen F, Dandou A, Fortuniak K, Gouvea ML, Hamdi R, Hendry M, Kawai T, Kawamoto Y, Kondo H, Krayenhoff ES, Lee SH, Loridan T, Martilli A, Masson V, Miao S, Oleson K, Pigeon G, Porson A, Ryu YH, Salamanca F, Shashua-Bar L, Steeneveld GJ, Tombrou M, Voogt J, Young D, Zhang N. 2010. The international urban energy balance models comparison project: first results from phase 1. *Journal of Applied Meteorology and Climatology* **49**: 1268–1292, DOI:10.1175/2010JAMC2354.1.

Hamilton IG, Davies M, Steadman P, Stone A, Ridley I, Evans S. 2009. The significance of the anthropogenic heat emissions of London's buildings: a comparison against captured shortwave solar radiation. *Building and Environment* **44**: 807–817, DOI: 10.1016/j.buildenv.2008.05.024.

Harrison R, McGoldrick B, Williams CGB. 1984. Artificial heat release from Greater London, 1971–1976. *Atmospheric Environment* **18**: 2291–2304, DOI:10.1016/0004-6981(84)90001-5.

ISO 8996. 2004. *Ergonomics of the Thermal Environment – Determination of Metabolic Heat Production*, International Organization for Standardization: Geneva, Switzerland.

Jacoby WG. 2000. Loess: a nonparametric, graphical tool for depicting relationships between variables. *Electoral Studies* **19**: 577–613, DOI:10.1016/S0261-3794(99)00028-1.

Jones WP. 2001. *Air Conditioning Engineering*, 5th edn. Butterworth-Heinemann: Oxford and Boston.

Kikegawa Y, Genchi Y, Yoshikado H, Kondo H. 2003. Development of a numerical simulation system toward comprehensive assessments of urban warming countermeasures including their impacts upon the urban buildings' energy-demands. *Applied Energy* **76**: 449–466, DOI:10.1016/S0306-2619(03)00009-6

Knight I, Dunn G. 2002. A/C energy efficiency in UK office environment. Proceedings of 2nd International Conference on Electricity Efficiency in Commercial Buildings, 27–29 May 2002, Nice, France.

Moriwaki R, Senoh H, Kanda M, Hagishima A, Kinouchi T. 2008. Anthropogenic water vapor emissions in Tokyo. *Water Resources Research* **44**: W11424, DOI:10.1029/2007WR006624.

Mosteller RD. 1987. Simplified calculation of body surface area. *New England Journal of Medicine* **317**: 1098–1098.

Narumi D, Kondo A, Shimoda Y. 2009. Effects of anthropogenic heat release upon the urban climate in a Japanese megacity. *Environmental Research* **109**: 421–431, DOI:10.1016/j.envres.2009.02.013.

Offerle B, Grimmond CSB, Fortuniak K. 2005. Heat storage and anthropogenic heat flux in relation to the energy balance of a central European city centre. *International Journal of Climatology* **25**: 1405–1419, DOI: 10.1002/joc.1198.

Psiloglou BE, Giannakopoulos C, Majithia S. 2007. Comparison of energy load demand and thermal comfort levels in Athens, Greece, and London, UK. Proceedings of 2nd PALENC Conference and 28th AIVC Conference on Building Low Energy Cooling and Advanced Ventilation Technologies in the 21st Century, Crete island, Greece. Vol. 2, 806–810.

Sailor DJ, Lu L. 2004. A top-down methodology for developing diurnal and seasonal anthropogenic heating profiles for urban areas. *Atmospheric Environment* **38**: 2737–2748, DOI: 10.1016/j.atmosenv.2004.01.034.

Sailor DJ, Brooks A, Hart M, Heiple S. 2007. A bottom-up approach for estimating latent and sensible heat emissions from anthropogenic sources. Proceedings of 7th Symposium on the Urban Environment, San Diego, CA.

Sailor DJ. 2011. A review of methods for estimating anthropogenic heat and moisture emissions in the urban environment. *International Journal of Climatology* **31**: 189–299, DOI: 10.1002/joc.2106.

Smith C, Lindley S, Levermore G. 2009. Estimating spatial and temporal patterns of urban anthropogenic heat fluxes for UK cities: the case of Manchester. *Theoretical and Applied Climatology* **98**: 19–35, DOI: 10.1007/s00704-008-0086-5.

Stanford HW, III. 2003. *HVAC Water Chillers and Cooling Towers*. Marcel Dekker: New York.

Taha H. 1997. Urban climates and heat islands: albedo, evapotranspiration and anthropogenic heat. *Energy and Buildings* **25**: 99–103, DOI:10.1016/S0378-7788(96)00999-1

Zhang X, Friedl MA, Schaaf CB, Strahler AH. 2004. The footprint of urban climates on vegetation phenology. *Geophysical Research Letters* **31**: L12209, DOI:10.1029/2004GL020137.

